the FEBS Journal

On the mechanisms of bananin activity against severe acute respiratory syndrome coronavirus

Zai Wang[1], Jian-Dong Huang[1], Kin-Ling Wong[2], Pei-Gang Wang[3], Hao-Jie Zhang[2], Julian A. Tanner[1], Ottavia Spiga[4,5], Andrea Bernini[4,5], Bo-Jian Zheng[2] and Neri Niccolai[4,5]

1 Department of Biochemistry, Faculty of Medicine, University of Hong Kong, China
2 Department of Microbiology, Faculty of Medicine, University of Hong Kong, China
3 The HKU-Pasteur Research Centre (HKU-PRC), Pokfulam, Hong Kong SAR, China
4 Department of Molecular Biology, University of Siena, Italy
5 SienaBiografix Srl, Siena, Italy

Keywords
antiviral drugs; bananin; coronavirus; viral helicase

Correspondence
J.-D. Huang or N. Niccolai, Department of Biochemistry, University of Hong Kong, 3/F Laboratory Block, Faculty of Medicine Building, 21 Sassoon Road, Pokfulam, Hong Kong SAR, China; Department of Molecular Biology, University of Siena, I-53100 Siena, Italy
Fax: +852 2855 1254; +39 0577 234903
Tel: +852 2819 2810; +39 0577 234910
E-mail: jdhuang@hkucc.hku.hk; niccolai@unisi.it

(Received 28 June 2010, revised 9 November 2010, accepted 12 November 2010)

doi:10.1111/j.1742-4658.2010.07961.x

In a previous study, severe acute respiratory syndrome coronavirus (SARS-CoV) was cultured in the presence of bananin, an effective adamantane-related molecule with antiviral activity. In the present study, we show that all bananin-resistant variants exhibit mutations in helicase and membrane protein, although no evidence of bananin interference on their mutual interaction has been found. A structural analysis on protein sequence mutations found in SARS-CoV bananin-resistant variants was performed. The S259/L mutation of SARS-CoV helicase is always found in all the identified bananin-resistant variants, suggesting a primary role of this mutation site for bananin activity. From a structural analysis of SARS-CoV predicted helicase structure, S259 is found in a hydrophilic surface pocket, far from the enzyme active sites and outside the helicase dimer interface. The S/L substitution causes a pocket volume reduction that weakens the interaction between bananin and SARS-CoV mutated helicase, suggesting a possible mechanism for bananin antiviral activity.

Introduction

At the beginning of the 21st Century, a novel virus, the severe acute respiratory syndrome coronavirus (SARS-CoV), moved into the human population causing SARS with a high rate of mortality. Although the last reported epidemic of SARS dates back to April 2004, the fact that this virus can replicate in a large number of animals, including dogs, cats, pigs, mice, ferrets, foxes, monkeys and rats [1–3], in addition to the natural hosts comprising Chinese palm civets, raccoon-dogs and bats [4–6], is of particular concern, suggesting that preparedness with vaccines and antiviral drugs against this potentially re-emerging agent is necessary.

It has been shown that treatment with ribavirin and corticosteroids as possible drugs against SARS-CoV only had slight beneficial effects or even enhanced viral replication in mice [7,8]. Thus, development of new anti-SARS drug is urgently needed for the potential SARS re-emergence. The relative conservation and essentialness in functionality of a particular gene are used as indicators to evaluate a drug target. On the basis of these criteria, helicase is a good target, being a

Abbreviations
NCBI, National Center for Biotechnology Information; PDB, Protein Data Bank; SARS, severe acute respiratory syndrome; SARS-CoV, SARS coronavirus.

relatively conserved protein in SARS-CoV (e.g. a less variable protein compared to spike protein) and critical for viral replication [9]. Accordingly, the latter protein has been proposed as an attractive target for anti-SARS research [10], in analogy with the promising results obtained for herpes simplex virus-1 [11,12].

In the present study, a structurally driven investigation for the design of new SARS-CoV helicase inhibitors is performed by correlating the predicted enzyme structure [13] with the observed bananin activity against SARS-CoV [14]. Bananins are a class of compounds with a unique structural signature incorporating a trioxa-adamantane moiety covalently bound to a pyridoxal derivative to add potential cytoprotective functionality [15]. Several parent adamantane derivatives are already used clinically [16,17], although the antiviral activity of the newly developed bananin has not yet been investigated extensively. *In vitro* assays demonstrated that bananin effectively interferes with SARS-CoV ATPase activity by inhibiting helicase activity. Furthermore, in a cell culture system of SARS-CoV, bananin inhibited viral replication at a half maximal effective concentration of less than 10 μM and a concentration causing 50% of cell death of over 300 μM, suggesting that it represents a promising anti-viral drug candidate [10]. To investigate bananin primary targets, bananin-resistant viruses were selected by culturing SARS-CoV (GZ50 strain; GenBank accession number AY304495) on fetal rhesus monkey kidney cell line FRhK-4 in the presence of high concentrations of this adamantine derivative. The half maximal effective concentration of bananin on these mutant viruses was demonstrated to be more than 50 μM. Mutations were found in helicase (S259L), membrane protein (A68V and R124W) and spike proteins (N479I). The trans-expression of mutant helicase or membrane protein during wild-type virus infection can rescue viral replication in the presence of bananin, demonstrating that the SARS-CoV helicase and M proteins were effective drug targets [14].

The present study describes the systematic search for those mutations found in bananin-resistant SARS-CoV variants. Subsequently, structural and functional results are compared to define the possible mechanisms of bananin activity, and are also used to drive restrained docking simulations of the bananin–SARS-CoV helicase interaction, aiming to define the sterical requirements of new antiviral drugs.

Results and Discussion

All the mutations found in the isolated bananin-resistant SARS-CoV variants are summarized in Table 1.

Table 1. Mutations in bananin-resistant virus variants. S, spike protein; M, membrane protein; NT, not tested.

Variants	Helicase	S	M
B15	S259L	N479I	A68V, R124W
B18	S259L, L297L/F	NT	A68V, R124W
B6, B14	S259L	NT	A68V, R124W
Other nine variants	S259L	NT	NT

Of primary relevance is the fact that the S259L mutation in helicase is always present, as well as the A68V and R124W mutations in membrane protein. This finding initially suggested that the observed antiviral activity could arise from bananin interference on a hypothetical helicase–membrane protein interaction, as in the case of the closely-related coronavirus mouse hepatitis virus, where the replicase protein complex including helicase colocalizes with M in the endoplasmic reticulum-Golgi intermediate compartment for virion packaging [18]. Thus, co-immunofluorescense and co-immunoprecipitation experiments were performed, although no evidence of helicase–membrane protein interaction could be obtained (Doc. S1 and Fig. S1). Thus, the mechanisms of bananin activity have been ascribed to the binding of the small molecule to single viral proteins and, in particular, to those exhibiting mutations in the bananin resistant SARS-CoV variants.

As shown in Table 1, mutations in spike protein, helicase and membrane protein have been detected. By using SCORECONS software [19], which quantifies residue conservation in multiple sequence alignments, Shannon's entropies have been calculated for each of the SARS-CoV protein sequence positions where mutations have been observed. In the case of SARS-CoV spike protein sequence, Shannon's entropy (in the range from 0 for invariant to 1 for hypervariable protein sequence positions) reveals that the 479 position, where the N/I mutation is found, corresponds to a highly variable site. A Shannon's entropy value of 0.72 is obtained by retrieving all of the 92 complete sequences of SARS-CoV spike protein present in the National Center for Biotechnology Information (NCBI) databases. The fact that bananin does not target on SARS-CoV entry (Doc. S1 and Fig. S2), suggests that no bananin-related activity can be attributed to the N479I mutation.

For the SARS-CoV membrane protein, only secondary structure predictions can be obtained, limiting a detailed structural interpretation of the functional roles of A68V and R124W mutations. BLAST analysis on the 19 complete sequences present in the NCBI databases for the SARS-CoV membrane protein suggests that the observed conservative substitution A68V is also encountered in two native viral clones (i.e. dbj_BAE93405 and

gb_AAP33701). From a structural point of view, the A68V mutation, occurring in a predicted protein trans-membrane region, should exhibit only a minor functional relevance. The case is different for the R124W mutation, which is outside the trans-membrane segments, with the arginyl residue being very conserved in all the available related sequences. Thus, the zero Shannon's entropy value calculated for the totally invariant 124 position of the membrane protein sequence suggests some functional role for such R/W replacement. However, the absence of tertiary structure information for the SARS-CoV membrane protein prevents further functional analysis of the R124W mutation.

The fact that tertiary and quaternary structures can be predicted for SARS-CoV helicase [13] allows a deeper insight into the function/structure correlations for native and mutated forms of the viral enzyme. Preliminary analysis on the frequency of amino acid substitutions among the 78 complete sequences of SARS-CoV helicase available from the NCBI databases indicates that S259 and L297 are totally conserved sites. Therefore, it can be suggested that chemical pressure as a result of the presence of bananin in cell cultures is the only driving force for selecting the observed mutations.

Functional validation for the helicase tertiary structure shown in Fig. 1 (atomic coordinates are available from the Protein Model Databank at http://www.caspur.it/PMDB under the accession number PM0076418) is provided by the observation that, in studies performed *in vivo*, S259/L and L297/F mutations do not interfere with viral metabolism because mutant virus variants carrying these two point mutations exhibited normal replication, as in the wild-type virus [14]. Of primary relevance is the fact that both S259 and L297 are predicted to be outside the surface regions where DNA binding, NTPase activity and dimerization occur. Moreover, it is interesting to note that L297, replaced by a phenylalanyl residue, is totally buried in the helicase structure, and that the conservative L/F substitution [20,21] does not cause any major changes in the helicase core structure.

A structural comparison of molecular models obtained for wild-type SARS-CoV helicase and the two bioactive mutants indicates how the replacement of S259 with the leucyl bulky side chain determines a volume decrease of a hydrophilic pocket present on the helicase surface. This surface pocket, formed by N257 and I258 backbone atoms together with S259, D260 and E261 side chains in the wild-type helicase (Fig. 2), reduces its volume from 253.45 to 211.40 Å^3

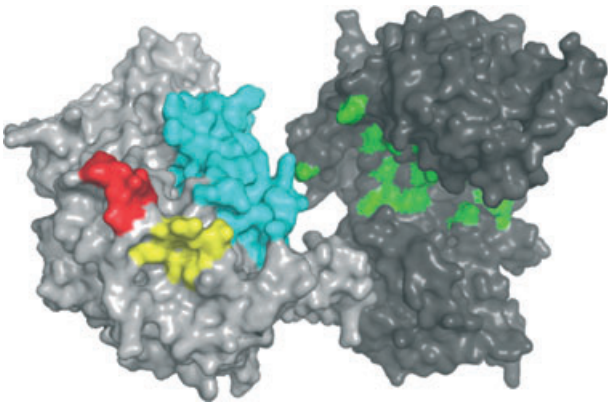

Fig. 1. Predicted quaternary structure of SARS-CoV helicase dimer. On each monomer surface, and colored with different gray scales, metal-binding domains, DNA duplex, ATP and bananin have been highlighted, respectively, in cyan, green, red and yellow.

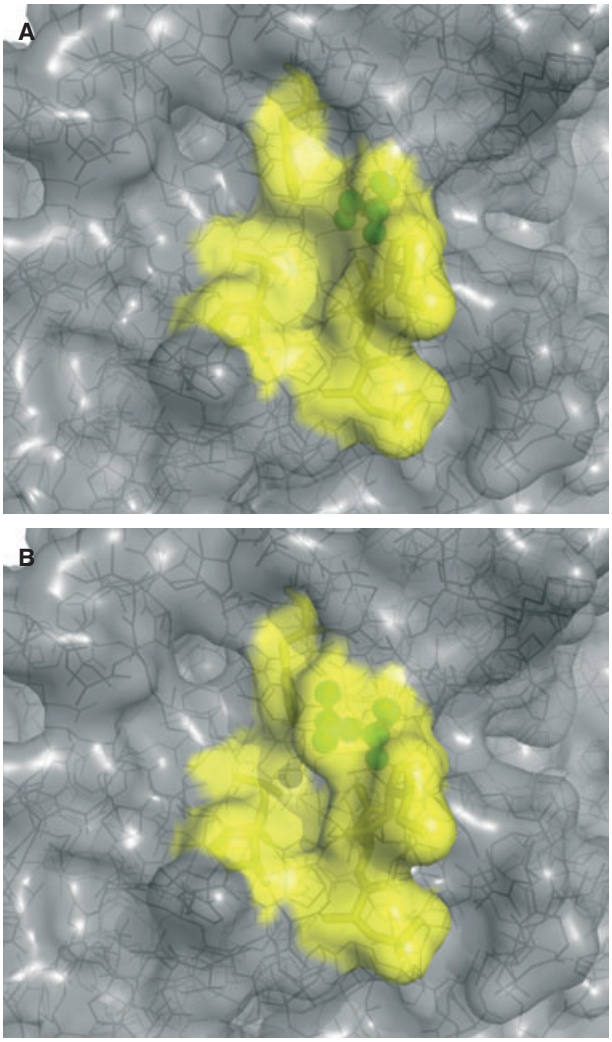

Fig. 2. Predicted bananin binding pocket of SARS-CoV helicase (A) in wild-type and (B) bananin-resistant variants. Seryl and leucyl side chains in position 259 are shown in a green ball and stick representation.

upon S/L replacement. In the case that the latter hydrophilic pocket of SARS-CoV helicase is the bananin binding site, the S/L mutation weakens the intermolecular interaction by reducing the number of possible hydrogen bond formations.

Electrostatic potential analysis for wild-type and S259/L mutant forms of SARS-CoV helicase was also carried out. As shown in Fig. 3, identical surfaces charge distributions are obtained, and therefore no electrostatic effects on helicase dimerization or helicase-DNA interaction can be attributed to the latter mutation. Furthermore, complementarity of positive and negative charges at the dimer interface region is apparent, supporting the reliability of the SARS-CoV helicase predicted structure.

Quantitative evaluation of S259/L mutation effects on bananin-SARS-CoV helicase binding has been performed with docking simulations on wild-type and mutated forms of the viral enzyme. In Fig. 4, the modes of bananin interaction with wild-type helicase are shown according to the results obtained from the docking simulation procedure. Thus, it is apparent how surface pockets of native and S/L mutated helicases are differently filled by bananin because binding with the small molecule involves a larger molecular interface in the case of the former helicase. Furthermore, the absence of the S259 OH group in the mutated viral enzyme prevents the formation of one hydrogen bond with bananin, accounting for the reduced strength of the bananin–helicase interaction.

Explanations of drug activity are usually provided by conformational changes in the targeted protein or by competitive binding at the protein active site. Alternative mechanisms of bananin antiviral activity have to be found because its protein target at the 259 sequence position presents a fully exposed side chain, and hence only limited local conformational rearrangements should result from the S/L mutation. Moreover, the fact that this mutation site is very far from the active site suggests that S259 is located either in an allosteric site of the enzyme or in a critical position for the overall protein flexibility. The fact that the S259/L helicase mutant is fully active is consistent with the above hypothesis proposing that this amino acid substitution, which is critical for bananin binding, does not interfere in the interaction of the enzyme with its natural substrates. The presence of the leucyl side chain in the protein mutant appears to cause steric hindrance to bananin binding, leaving the traffic of water molecules in and out from the hydrophilic pocket almost unaffected. Removal of such water molecules upon bananin binding could reduce helicase flexibility, which a very critical feature for the activity of this class of enzymes [22].

Thus, it can be concluded that bananin resistant SARS-CoV variants have delineated an overall protein mutation pattern indicating the critical role of the helicase S259/L mutation. The possibility that bananin binding to S259 reduces the enzyme activity affecting helicase dynamics is consistent with the observed bananin-resistance of SARS-CoV variants containing S259/L helicase mutations. These results are useful with respect to the rational design of new anti-SARS-CoV drugs in the event of a new unexpected pandemic.

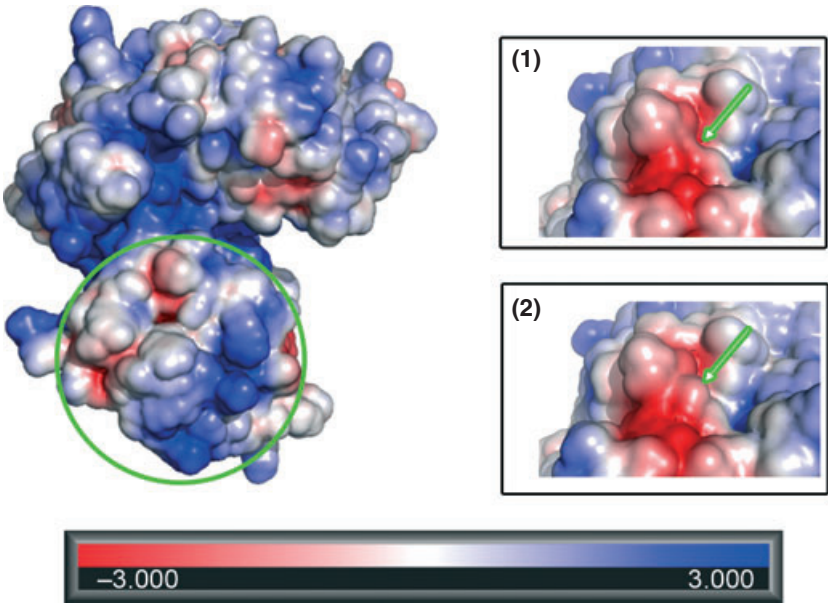

Fig. 3. Electrostatic potential distribution of SARS-CoV helicase: the basic (dark blue coloured) region involved in DNA binding and the dimer interface (circled in green) are shown. On the opposite side of the protein, S259/L regions in the wild-type (inset 1) and mutated form (inset 2) of the viral enzyme are also shown.

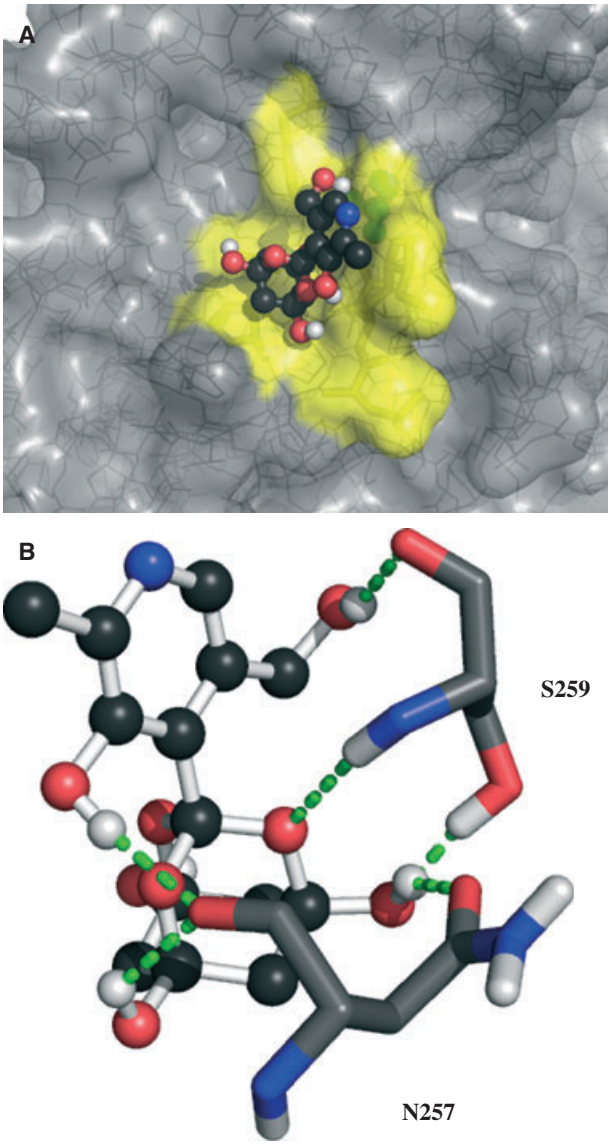

Fig. 4. Lowest energy structure of the wild-type SARS-CoV helicase-bananin complex obtained from the docking simulation (A). Bananin hydrogen bond network with helicase donor/acceptor moieties are also shown (B).

Experimental procedures

Generation of bananin-resistant virus

SARS-CoV strain GZ50 [23] was cultured on FRhK-4 cells. This cell line was used to isolate and culture this virus strain from the very beginning, and was considered fully permissive for viral replication [10,14]. SARS-CoV was cultured in the presence of 50 μM bananin for four passages and then 100 μM bananin for an additional four passages. The bananin-resistant virus variants were identified by a plaque assay in the presence of 100 μM bananin as described previously [24] and further isolated by isolating viral plaques.

Sequencing of mutant virus genome

Fourteen pairs of primers were designed according to GZ50 sequence for PCR amplification of the whole genome of mutant SARS-CoV. Each agarose gel purified a fragment of approximately 2 kb that was used as a template for the sequencing reaction. PCR primers and sequencing primers are available upon enquiry.

Protein sequence analysis

Protein sequences of SARS-CoV helicase (SP_P59641), spike (SP_P59594) and membrane (SP_P59596) proteins were retrieved from SwissProt Database. Sequence alignments of these three proteins with all SARS coronavirus sequences were obtained with CLUSTALW, version 1.8 [25], and analyzed in terms of sequence variability by using the SCORECONS server [19]. Shannon's sequence entropies were considered as a quantitative measure of residue conservation.

Molecular modeling

The predicted structure of SARS-CoV helicase, taken from the Protein Data Bank (PDB) with the PDB ID code 2G1F [13], was used as the initial reference structure. By using GROMACS software [26], ten cycles of simulated annealing of 500 ps each were carried out to improve side chain packing and to remove most of the stereochemical ambiguities present in the selected PDB file. Similarly, the structures of helicase S/L and L/F mutants were obtained, and the atomic coordinates of the lowest energy structures of the wild-type form of SARS-CoV helicase are available from the Protein Model Databank (http://www.caspur.it/PMDB) under accession number PM0076418. By structural homology with other helicase dimers and helicase-DNA adducts (PDB ID codes 1UAA, 3PJR and 2IS1), the interface between SARS-CoV helicase and DNA has also been predicted. The structure of bananin (i.e. 1-[3-hydroxy-5-(hydroxymethyl)-2-methyl-4-pyridinyl]-2,8,9-trioxaadamantane-3,5,7-triol) was parameterized by using MOPAC2007 [27]. Volumes of the proposed bananin binding pocket of native and mutated SARS-CoV helicases were measured using the online tool CASTP (http://cast.engr.uic.edu) [28]. ADAPTIVE POISSON–BOLTZMANN SOLVER software was used for evaluating the electrostatic properties of SARS-CoV helicase [29]. Figures were prepared with PYMOL using PDB2PQR [30,31].

Docking simulations

AUTODOCK 4.0 was used to simulate a flexible docking process for the interaction of bananin with SARS-CoV helicase and to analyze their binding modes [32]. The AUTODOCK

tool (ADT) was used to optimize ligand and protein by adding polar hydrogens and loading Kollman united atoms charges, as well as to perform docking calculations. A grid box with dimensions $40 \times 40 \times 58$ points was constructed around the SARS-CoV helicase S259 residue. All bond rotations and torsions for bananin were automatically set by the ADT routine. The Lamarckian genetic algorithm procedure was employed and the docking runs were set to 250 and a maximum number of 2 500 000 energy evaluations. In the docking simulations, all the other parameters were set to defaults. The resulting orientations with rmsd ≤ 0.5 Å were clustered.

Acknowledgements

Bananin was kindly provided by Dr A. J. Kesel (Chammünsterstrasse 47, D81827 München, Germany). This work was supported by grants (01030182 and 02040192) from the Research Fund for the Control of Infectious Diseases (RFCID) awarded to Dr J. D. Huang and by grants from the University of Siena.

References

1 Chen W, Yan M, Yang L, Ding B, He B, Wang Y, Liu X, Liu C, Zhu H, You B *et al.* (2005) SARS-associated coronavirus transmitted from human to pig. *Emerg Infect Dis* **11**, 446–448.
2 Martina BE, Haagmans BL, Kuiken T, Fouchier RA, Rimmelzwaan GF, Van Amerongen G, Peiris JS, Lim W & Osterhaus AD (2003) Virology: SARS virus infection of cats and ferrets. *Nature* **425**, 915.
3 Shi Z & Hu Z (2008) A review of studies on animal reservoirs of the SARS coronavirus. *Virus Res* **133**, 74–87.
4 Guan Y, Zheng BJ, He YQ, Liu XL, Zhuang ZX, Cheung CL, Luo SW, Li PH, Zhang LJ, Guan YJ *et al.* (2003) Isolation and characterization of viruses related to the SARS coronavirus from animals in southern China. *Science* **302**, 276–278.
5 Song HD, Tu CC, Zhang GW, Wang SY, Zheng K, Lei LC, Chen QX, Gao YW, Zhou HQ, Xiang H *et al.* (2005) Cross-host evolution of severe acute respiratory syndrome coronavirus in palm civet and human. *Proc Natl Acad Sci USA* **102**, 2430–2435.
6 Lau SK, Woo PC, Li KS, Huang Y, Tsoi HW, Wong BH, Wong SS, Leung SY, Chan KH & Yuen KY (2005) Severe acute respiratory syndrome coronavirus-like virus in Chinese horseshoe bats. *Proc Natl Acad Sci USA* **102**, 14040–14045.
7 Lau AC, So LK, Miu FP, Yung RW, Poon E, Cheung TM & Yam LY (2004) Outcome of coronavirus-associated severe acute respiratory syndrome using a standard treatment protocol. *Respirology* **9**, 173–183.
8 Barnard DL, Day CW, Bailey K, Heiner M, Montgomery R, Lauridsen L, Winslow S, Hoopes J, Li JK, Lee J *et al.* (2006) Enhancement of the infectivity of SCVin BALB/c mice by IMP dehydrogenase inhibitors, including ribavirin. *Antiviral Res* **71**, 53–63.
9 Van Dinten LC, Van Tol H, Gorbalenya AE & Snijder EJ (2000) The predicted metal-binding region of the arterivirus helicase protein is involved in subgenomic mRNA synthesis, genome replication, and virion biogenesis. *J Virol* **74**, 5213–5223.
10 Tanner JA, Zheng BJ, Zhou J, Watt RM, Jiang JQ, Wong KL, Lin YP, Lu LY, He ML, Kung HF *et al.* (2005) The adamantane-derived bananins are potent inhibitors of the helicase activities and replication of SARS coronavirus. *Chem Biol* **12**, 303–311.
11 Crute JJ, Grygon CA, Hargrave KD, Simoneau B, Faucher AM, Bolger G, Kibler P, Liuzzi M & Cordingley MG. (2002) Herpes simplex virus helicase-primase inhibitors are active in animal models of human disease. *Nat Med* **8**, 386–391.
12 Kleymann G, Fischer R, Betz UA, Hendrix M, Bender W, Schneider U, Handke G, Eckenberg P, Hewlett G, Pevzner V *et al.* (2002) New helicase-primase inhibitors as drug candidates for the treatment of herpes simplex disease. *Nat Med* **8**, 392–398.
13 Bernini A, Spiga O, Venditti V, Prischi F, Bracci L, Huang J, Tanner JA & Niccolai N (2006) Tertiary structure prediction of SARS coronavirus helicase. *Biochem Biophys Res Commun* **343**, 1101–1104.
14 Huang JD, Zheng BJ & Sun HZ (2008) Helicases as antiviral drug targets. *Hong Kong Med J* **14**, 36–38.
15 Kesel AJ (2003) A system of protein target sequences for anti-RNA-viral chemotherapy by a vitamin B_6-derived zinc-chelating trioxa-adamantane-triol. *Bioorg Med Chem* **11**, 4599–4613.
16 Davies WL, Grunert RR, Haff RF, McGahen JW, Neumayer EM, Paulshockm M, Watts JC, Wood TR, Hermann EC & Hoffmann CE (1964) Antiviral activity of 1-adamantanamine (amantadine). *Science* **144**, 862–863.
17 Schwab RS, England AC, Poskanzer DC & Young RR (1969) Amantadine in the treatment of Parkinson's disease. *JAMA* **208**, 1168–1170.
18 Bost AG, Prentice E & Denison MR (2001) Mouse hepatitis virus replicase protein complexes are translocated to sites of M protein accumulation in the ERGIC at late times of infection. *Virology* **285**, 21–29.
19 Valdar WSJ (2002) Scoring residue conservation. *Proteins* **43**, 227–241.
20 Dayhoff MO, Schwartz RM & Orcutt BC (1978) A model of evolutionary change in proteins. In *Atlas of Protein Sequence and Structure* (Dayhoff MO, eds), vol 5, pp. 345–352. Nat. Biomed. Res. Found., Washington, DC.

21 Le SQ & Gascuel O (2008) An improved general amino acid replacement matrix. *Mol Biol Evol* **25**, 1307–1320.
22 Yang W (2010) Lessons Learned From UvrD Helicase: mechanism for directional movement. *Annu Rev Biophys* **39**, 367–385.
23 Zhong NS, Zheng BJ, Li YM, Poon LLM, Xie ZH, Li PH, Tan SY, Chang Q, Xie JP, Liu XQ *et al.* (2003) Epidemiology and cause of severe acute respiratory syndrome (SARS) in Guangdong, People's Republic of China, in February. *Lancet* **362**, 1353–1358.
24 Kao RY, Tsui WH, Lee TS, Tanner JA, Watt RM, Huang JD, Hu L, Chen G, Chen Z, Zhang L *et al.* (2004) Identification of novel small-molecule inhibitors of severe acute respiratory syndrome-associated coronavirus by chemical genetics. *Chem Biol* **11**, 1293–1299.
25 Thompson JD, Higgins D & Gibson TJ (1994) CLUSTAL W: improving the sensitivity of progressive multiple sequence alignment through sequence weighting, position-specific gap penalties and weight matrix choice. *Nucleic Acids Res* **22**, 4673–4680.
26 Lindahl E, Hess B & Van der Spoel D (2001) GROMACS 3.0: a package for molecular simulation and trajectory analysis. *J Mol Model* **7**, 306–317.
27 Rocha GB, Freire RO, Simas AM & Stewart JJ (2006) RM1: a reparameterization of AM1 for H, C, N, O, P, S, F, Cl, Br, and I. *J Comput Chem* **27**, 1101–1111.
28 Dundas J, Ouyang Z, Tseng J, Binkowski A, Turpaz Y & Liang J (2006) CASTp: computed atlas of surface topography of proteins with structural and topographical mapping of functionally annotated resiudes. *Nucleic Acids Res* **34**, 116–118.
29 Baker NA, Sept D, Joseph S, Holst MJ & McCammon JA (2001) Electrostatic of nanosystems: applications to microtubules and the ribosome. *Proc Natl Acad Sci USA* **98**, 10037–10041.
30 Dolinsky TJ, Nielsen JE, McCammon JA & Baker NA (2004) PDB2PQR: an automated pipeline for the setup of Poisson-Boltzmann electrostatics calculations. *Nucleic Acids Res* **32**, 665–667.
31 DeLano WL (2002) *The PyMOL molecular Graphics System*. DeLano Scientific, San Carlos, http://www.pymol.org.
32 Morris GM, Goodsell DS, Halliday RS, Huey R, Hart WE, Belew RK & Olson AJ (1998) Automated docking using a Lamarckian genetic algorithm and empirical binding free energy function. *J Comput Chem* **19**, 1639–1662.

Supporting information

The following supplementary material is available:
Doc. S1. Supplementary material.
Fig. S1. No interactions between SARS-CoV helicase and M proteins.
Fig.S2. Bananin has no effect on HIV/SCV pseudotyped viral entry.

This supplementary material can be found in the online version of this article.

Please note: As a service to our authors and readers, this journal provides supporting information supplied by the authors. Such materials are peer-reviewed and may be re-organized for online delivery, but are not copy-edited or typeset. Technical support issues arising from supporting information (other than missing files) should be addressed to the authors.